

Supporting information for

Reduced linewidth multipolar plasmon resonances in metal nanorods and related applications

Shunping Zhang^{ab}, Li Chen^{ac}, Yingzhou Huang^d and Hongxing Xu^{*abe}

^a*Beijing National Laboratory for Condensed Matter Physics and Institute of Physics,
Chinese Academy of Sciences, Box 603-146, Beijing 100190, China*

^b*Center for Nanoscience and Nanotechnology, and School of Physics and Technology,
Wuhan University, Wuhan 430072, China*

^c*Department of Applied Physics, Hunan University, Changsha 410082, China*

^d*Department of Applied Physics, Chongqing University, Chongqing 400044, China*

^e*Division of Solid State Physics/The Nanometer Structure Consortium, Lund
University, Box 118, S-22100, Lund, Sweden*

*Corresponding author. Email: hxxu@iphy.ac.cn

More examples of dark-field scattering spectra of Ag nanorods are shown in Figs. S1-S4. For long nanorods as shown in Figs. S3 and S4, most of the spectra show a decrease in the peak intensity for LSPR in the near IR region. This is likely due to a reduction in the collection efficiency of the spectrometer. The image of a long nanorod in the plane where a slice is located is larger for longer wavelength due to the dispersion of the objective. Then, part of the scattered light from the nanorod would be cut by the slice so that the observed scattering intensity is reduced in the near IR region. Note that this would not be the case for shorter nanorods or for those long nanorods that have their images aligned parallel to the slice. This may explain why the behavior appears in most long nanorods but some of them are exception.

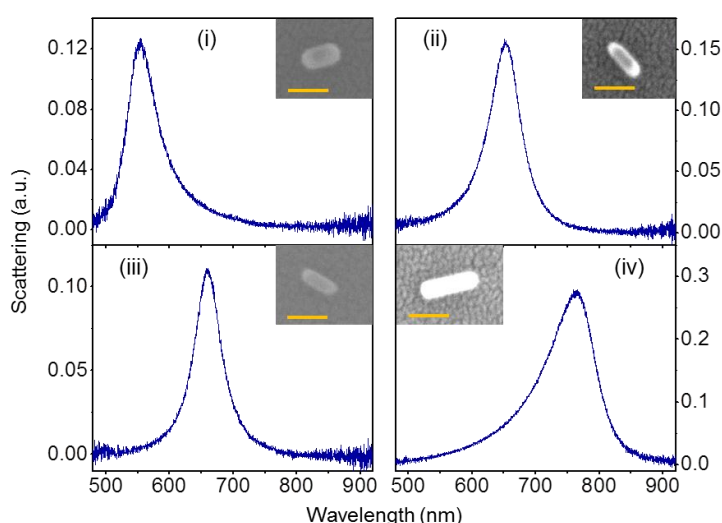


Fig. S1 Dark-field scattering spectra of single Ag nanorods: (i) $D = 41 \text{ nm}$, $L = 86 \text{ nm}$, (ii) $D = 26 \text{ nm}$, $L = 91 \text{ nm}$, (iii) $D = 24 \text{ nm}$, $L = 79 \text{ nm}$ and (iv) $D = 31 \text{ nm}$, $L = 135 \text{ nm}$. The SEM images of the corresponding rods are shown in the insets. The scale bars are 100 nm. The diameters and lengths of nanorods were measured from SEM images after subtracting 12 nm to account for the sputtered Au layer.

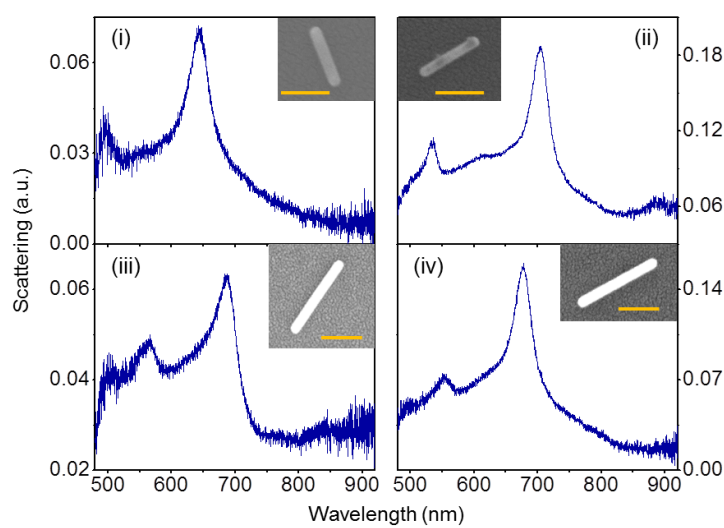


Fig. S2 Dark-field scattering spectra of single Ag nanorods: (i) $D = 38 \text{ nm}$, $L = 247 \text{ nm}$, (ii) $D = 30 \text{ nm}$, $L = 265 \text{ nm}$, (iii) $D = 38 \text{ nm}$, $L = 410 \text{ nm}$ and (iv) $D = 39 \text{ nm}$, $L = 427 \text{ nm}$. The SEM images of the corresponding rods are shown in the insets. The scale bars are 200 nm.

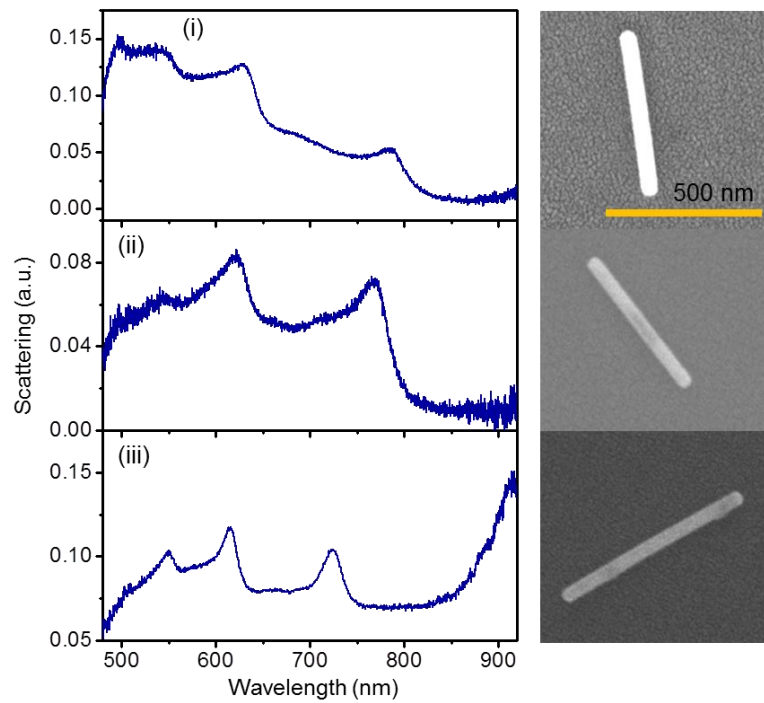


Fig. S3 Dark-field scattering spectra of single Ag nanorods: (i) $D = 44 \text{ nm}$, $L = 521 \text{ nm}$, (ii) $D = 35 \text{ nm}$, $L = 496 \text{ nm}$ and (iii) $D = 34 \text{ nm}$, $L = 649 \text{ nm}$. The SEM images of the corresponding rods are shown to the right. The scale bar applies to all three images.

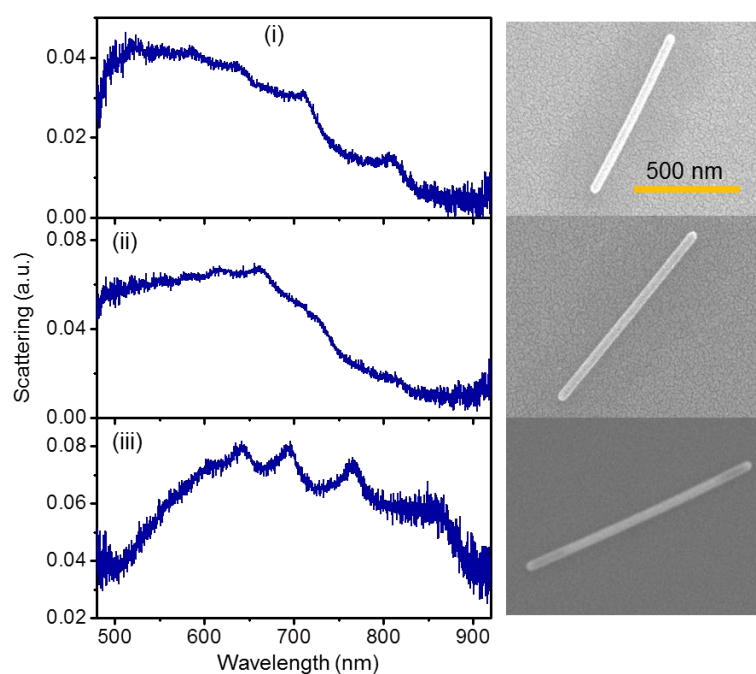


Fig. S4 Dark-field scattering spectra of single Ag nanorods: (i) $D = 32$ nm, $L = 821$ nm, (ii) $D = 34$ nm, $L = 1007$ nm and (iii) $D = 34$ nm, $L = 1155$ nm. The SEM images of the corresponding rods are shown to the right. The scale bar applies to all three images.

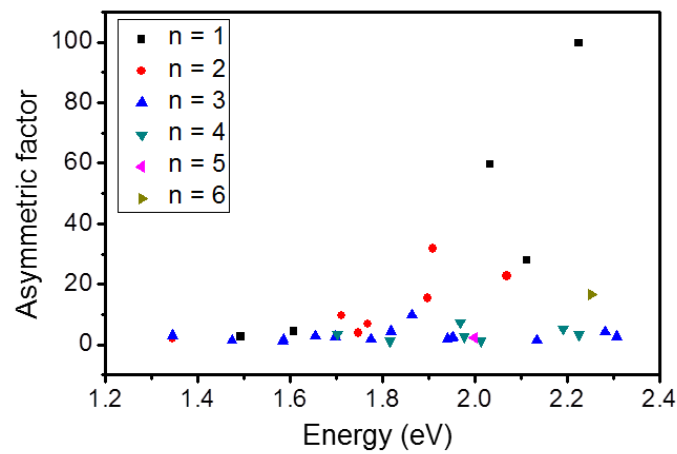


Fig. S5 Asymmetric factor q as a function of energy, obtained from the fits to the resonant peaks in the dark-field scattering spectra.